

- (10) L. Kotin and M. Nagasawa, *J. Chem. Phys.*, **36**, 873, (1962).
 (11) A. D. MacGillivray and J. J. Winkleman, Jr., *J. Chem. Phys.*, **45**, 2184 (1966).
 (12) A. D. MacGillivray, *J. Chem. Phys.*, **56**, 80, 83, (1972); **57**, 4071, 4075 (1972).
 (13) G. S. Manning, *J. Chem. Phys.*, **51**, 924, 3249 (1969); *Biophys. Chem.*, **7**, 95 (1977).
 (14) G. S. Manning and A. Holtzer, *J. Phys. Chem.*, **77**, 2206 (1973).
 (15) Z. Alexandrowicz, *J. Chem. Phys.*, **47**, 4377 (1967).
 (16) L. Onsager, *Ann. N.Y. Acad. Sci.*, **51**, 627 (1949). We are grateful to a referee for supplying an additional reference to D. Stigter, *Biopolymers*, **16**, 1435 (1977). Stigter corrects a derivation of the potential given by S. L. Brenner and V. A. Parsegian, *Biophys. J.*, **14**, 327 (1974), and obtains the result that we have given in eq II.10. We have retained our remarks concerning the derivation of eq II.10, in the belief that our elementary derivation may have some interest. Stigter should also be consulted for a plausible scaling of the Debye–Hückel interaction to account for “condensation”.
 (17) H. Yamakawa, “Modern Theory of Polymer Solutions”, Harper and Row, New York, N.Y., 1971.
 (18) M. Abramowitz and I. A. Stegun, “Handbook of Mathematical Functions”, Dover Publications, New York, N.Y., 1972.
 (19) H. Yamakawa and G. Tanaka, *J. Chem. Phys.*, **55**, 3188 (1971), and private communication.
 (20) G. E. Boyd and D. P. Wilson, *J. Phys. Chem.*, **80**, 805 (1975).
 (21) J. Skerjanc, *Biophys. Chem.*, **1**, 376 (1974).
 (22) T. Orofino and P. J. Flory, *J. Phys. Chem.*, **63**, 283 (1959).

Charge Interactions in Cylindrical Polyelectrolytes

J. Skolnick and M. Fixman*

Department of Chemistry, Yale University, New Haven, Connecticut 06520.

Received May 10, 1978

ABSTRACT: The Debye–Hückel equation is solved for the electrostatic interaction of point charges on the surface of a dielectric cylinder immersed in salt water. Numerical results are given for the potential as a function of axial separation for charges on the same side and on opposite sides of the cylinder, and for two values of the Debye screening length: infinity and unity, in units of the cylinder radius. Major deviations from the interaction in bulk solvent are found. The analytical results are also applied to the self-energy of a helical distribution of charge, and that part $\Delta\Psi$ of the self-energy which depends on salt concentration is isolated. The deviation of $\Delta\Psi$ from its value for a uniformly charged cylinder is evaluated as a function of screening length. The deviation is small for DNA, and smaller for the α helix. The deviation from a line of charge self-energy is much more significant, but all expressions for $\Delta\Psi$ agree if the salt concentration is low.

I. Introduction

Although linear polyelectrolytes have been extensively studied for many years, the influence of the low dielectric constant backbone on the potential of mean force between a charge on the polymer and another ion is not well understood. We have studied this potential on the basis of classical electrostatic theory, which is supplemented by Debye–Hückel screening. One would like to know under what conditions, if any, the backbone behaves as if it were electrostatically invisible.

We cannot hope to summarize the vast body of polyelectrolyte literature which in one way or another models the low dielectric constant effect; rather a brief review emphasizing the ideas that influenced the present work will be undertaken.

An early consideration of the effect of a local dielectric constant appears in the work of Kirkwood and Westheimer^{1,2} on the electrostatic influence of substituents on the dissociation constants of organic acids. The organic acid is treated as a spherical, and subsequently ellipsoidal, low dielectric constant region within which an arbitrary discrete collection of charges is located. The molecule is assumed to be immersed in salt-free, bulk solvent. Kirkwood and Westheimer express the electrostatic free energy in two parts: one part represents the Coulomb interaction of charges immersed in an infinite medium of dielectric constant characteristic of the molecule, and the other part gives boundary corrections. Buff et al.³ and Beveridge et al.⁴ have recently noted many related problems and devised several solutions for spherical boundaries. Harris and Rice⁵ considered spheres permeated by salt solution and included appropriate screening.

A wide class of polyelectrolytes is more appropriately modeled by cylindrical rather than spherical domains.

Hill⁶ has solved the linearized Poisson–Boltzmann, or Debye–Hückel equation, for a uniformly charged cylinder immersed in bulk solvent. The result appears in terms of modified Bessel functions, and will be displayed later. It is of interest to observe that the potential outside the cylinder is independent of the dielectric constant inside, as is the charging free energy. But there is no reason to assume a priori that the potential for a more realistic charge distribution will remain independent of the interior dielectric constant. Indeed, the latter turns out to have large effects on the potential of discrete charge distributions.

For discussions of charge condensation, we refer to the literature.^{7,8} Evidence exists that the linearized Poisson–Boltzmann equation describes the electrostatic potential outside the layer of condensed ions, and our use of that equation may therefore be consistent with condensation. But this work is concerned with a solution of the linearized equation, and not with its domain of application.

In section II the linearized Poisson–Boltzmann equation is solved for a discrete source charge located on the surface of a dielectric cylinder. The more general case is considered elsewhere.⁹ The cylinder is supposed impermeable to the salt solution in which it is immersed and to have a dielectric constant D_0 different from the bulk value D . The solution to this problem is equivalent to a determination of the interaction free energy between two charges, one of which is on the cylinder. Numerical results are given for the special case that both charges are on the surface of the cylinder, either on the same or on opposite sides, and separated by an axial distance z .

In section III helical charge distributions of arbitrary pitch are considered. The solution to this problem is relevant to the calculation of colligative properties, and

possibly also to the question of structural stability. Our numerical work has thus far been confined to the case of a continuous helical stripe. The difference between the electrostatic free energy of the uniform charge distribution and the helical stripe is found to be rather small for either the α helix or for DNA, but increases with increasing pitch and increasing salt concentration. Possibly the difference might be significant for DNA at high salt concentrations. However, the severe effect of the dielectric cylinder on the interaction between two point charges has a different sign depending on whether the charges are on the same or opposite sides of the cylinder, and there is evidently a major cancellation for a helical distribution.

Although the difference in potential between a helix distribution and a uniform distribution of surface charge is small, insofar as the dependence on salt concentration is concerned, the difference between a uniform surface distribution and a line of charge may be quite substantial. The latter is often used. Any reluctance to take this difference into account, on the grounds that the uniform surface distribution is too crude an approximation to the helix, should be reduced by our results.

II. The Potential of a Point Charge

The potential due to a unit point charge at r_0 on the surface of a cylinder will be evaluated in this section. The cylinder is supposed to exclude the salt solution in which it is immersed, to have a dielectric constant D_0 that may be different from that of the solution, namely D , and to be infinitely long. If the cylinder was absent, the potential would have the Debye-Hückel form $\exp(-\kappa|\mathbf{r} - \mathbf{r}_0|)/D|\mathbf{r} - \mathbf{r}_0|$.

The formal solution to the problem will be summarized below, in part A. Numerical results are presented in part B. Their calculation proved extremely annoying and required a combination of contour deformations, employment of asymptotic forms, and precautions with the numerical integration, all of which is discussed in the Appendix.

A. Formal Theory. The potential due to a point charge at r_0 is by definition the Green's function G , and is presumed to satisfy a Poisson-Boltzmann equation. Linearization according to the Debye-Hückel method gives

$$\nabla \cdot D(\mathbf{r}) \nabla G - \kappa^2(\mathbf{r}) D(\mathbf{r}) G = -4\pi\delta(\mathbf{r} - \mathbf{r}_0) \quad (\text{II.1})$$

where the dielectric constant and screening parameter are discontinuous across the boundary of the cylinder. In cylindrical polar coordinates (z, ρ, ϕ) , and for a cylinder of radius a (which will eventually be the unit of length), the discontinuous functions are

$$\begin{aligned} D(\mathbf{r}) &= D_0, \quad \kappa(\mathbf{r}) = \kappa_0 & \text{if } \rho < a \\ D(\mathbf{r}) &= D, \quad \kappa(\mathbf{r}) = \kappa & \text{if } \rho > a \end{aligned} \quad (\text{II.2})$$

In due course κ_0 will be put equal to zero (it proves helpful in the contour deformation to postpone this step). The following standard procedures reduced the problem to a one-dimensional one. First eq II.1 is written in cylindrical polar coordinates, and second a Fourier decomposition of the angular and z dependence is introduced. The source charge is at $\mathbf{r}_0 = (z_0, \rho_0, \phi_0) = (0, a, 0)$.

$$\delta(\phi) = (2\pi)^{-1} \sum_{m=-\infty}^{\infty} \exp(im\phi) \quad (\text{II.3})$$

$$\delta(z) = (2\pi)^{-1} \int_{-\infty}^{\infty} \exp(ikz) dk \quad (\text{II.4})$$

$$G = (2\pi)^{-2} \sum_{m=-\infty}^{\infty} \int_{-\infty}^{\infty} dk g_m \exp(im\phi + ikz) \quad (\text{II.5})$$

These equations and (II.1) determine that $g_m(\rho)$ must satisfy

$$\frac{1}{\rho} \frac{\partial}{\partial \rho} \left(\rho D(\rho) \frac{\partial g_m}{\partial \rho} \right) - D(\rho) \left(k^2 + \kappa^2(\rho) + \frac{m^2}{\rho^2} \right) g_m = -\frac{4\pi\delta(\rho - a)}{a} \quad (\text{II.6})$$

The potential g_m is continuous, and vanishes at infinity, but eq II.6 dictates a discontinuity in its derivative at the cylinder surface.

$$D(\partial g_m / \partial \rho)_+ - D_0(\partial g_m / \partial \rho)_- = -4\pi/a \quad (\text{II.7})$$

where the subscripts $+$ and $-$ designate limits as $\rho \rightarrow a$ from outside and inside the cylinder, respectively. Since eq II.6 reduces to Bessel's equation for the piecewise continuous parameters, we have¹⁰

$$\begin{aligned} g_m &= A_m I_m(l_0 a) K_m(l \rho), & \rho \geq a \\ g_m &= A_m I_m(l_0 \rho) K_m(l a), & \rho \leq a \end{aligned} \quad (\text{II.8})$$

where

$$l^2 = k^2 + \kappa^2; \quad l_0^2 = k^2 + \kappa_0^2 \quad (\kappa_0 \rightarrow 0) \quad (\text{II.9})$$

The boundary condition, eq II.7, readily determines A_m to be

$$a A_m = -4\pi [D l I_m(l_0 a) K_m'(l a) - D_0 l_0 I_m'(l_0 a) K_m(l a)]^{-1} \quad (\text{II.10})$$

It follows from eq II.5, II.8, and II.10 that the calculation has been reduced to numerical integration and summation. The results may be summarized as follows:

$$|z| G = H_0 + 2 \sum_{m=1}^{\infty} H_m \cos m\phi$$

$$\begin{aligned} H_m &\equiv (|z|/4\pi^2) \int_{-\infty}^{\infty} g_m \exp(ikz) dk = \\ &(|z|/2\pi^2) \int_0^{\infty} g_m \cos(kz) dk \end{aligned} \quad (\text{II.11})$$

and g_m is determined from eq II.8-II.10. Practical computation based on these formulas is still quite difficult for the following reasons. If z is small, the integration is numerically feasible, but the sum over m converges very slowly. If z is large the sum converges rapidly, but direct integration is not feasible. Also if ϕ is large, that is, if the potential is calculated on the opposite side of the cylinder from the source charge, then successive contributions to the sum alternate in sign, and rather high accuracy is required for meaningful results. The interested reader is referred to the Appendix for the resolution of these problems.

B. Numerical Results. Since our major goal is insight into the effects of the cylinder, rather than any specific application, we have specialized our numerical work to a few special cases. The two charges under consideration, test and source charges, are located on the surface of the cylinder at $\rho = 1$, and are either on the same side of the cylinder at $\phi = 0^\circ$, or are on opposite sides at $\phi = 180^\circ$. The value of κ is zero or unity; that is, the Debye screening length is either infinite or is one cylinder radius.

Limiting cases that are accessible analytically are $(z, \phi) \rightarrow (0, 0)$ and $z \rightarrow \infty$. The former case is equivalent to two charges on a planar dividing surface between two regions of different dielectric constant, and gives $zG \rightarrow 2/(D + D_0)$, for any κ . For large z the charge interaction reduces to the Debye-Hückel form, but approaches this form extremely slowly. (Indeed, the factor $1/z$ in the potential is probably not correct if salt is present. But the exponential factor

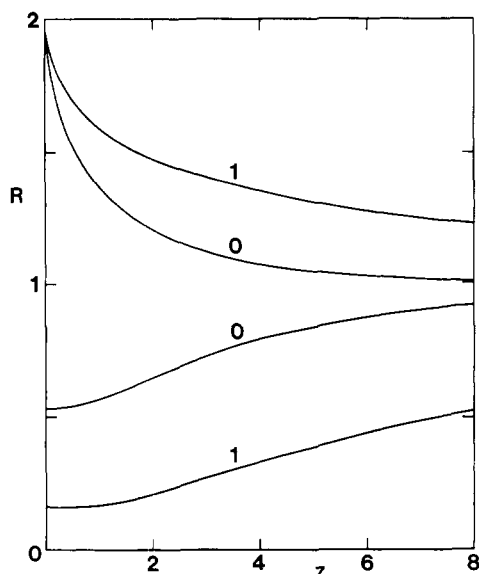


Figure 1. R is the actual electrostatic interaction between two charges on the surface of a cylinder divided by the interaction in bulk solvent of two charges separated by the same distance. z is the axial separation between the charges, in units of the cylinder radius. The cylinder has dielectric constant 2, and the bath 80. Values of the screening constant $\kappa = 0$ or 1 are indicated. The two curves with $R > 1$ refer to charges on the same side of the cylinder ($\phi = 0^\circ$), and the two curves with $R < 1$ refer to charges on opposite sides ($\phi = 180^\circ$).

then dominates the behavior at $z \rightarrow \infty$, and so it did not seem worthwhile to pursue the formal correction.)

Numerical results are shown in Figure 1 for the ratio of the actual interaction potential G to the Debye-Hückel potential as a function of z for the two values of κ and ϕ . We found the results for charges on opposite sides of the cylinder to be quite contrary to our naive expectations that the interaction would be greatly increased by the presence of a low dielectric constant region between the charges. On the contrary, the interaction is greatly decreased! We note that these results would not be changed by any small shift of the charges toward the interior of the cylinder, or toward the bulk solvent, because the potential is continuous across the dividing surface.

A rationalization along the following lines is probably acceptable. The lines of force from a charge avoid passing through the cylinder. If they passed through the interaction would indeed be increased over its value in bulk solution. Rather the lines of force avoid the cylinder and travel through the solution to a charge on the opposite side of the cylinder. The greater distance leads to a decreased flux density from spreading of the lines of flux, and from their termination on counterions. If the two charges are close together on the same side of the cylinder, the lines of force bunch up somewhat, and thereby increase the interaction.

At this point we wish to add two additional remarks stimulated by the extremely sceptical response of a referee toward our decreased interaction energy. Our first remark amplifies the physical meaning of the Green's function G , and our second remark concerns a second example, much easier to verify than the cylinder problem, of a reduction in charge interaction due to a foreign dielectric having $D_0 < D$, placed between two charges.

The Green's function $G(\mathbf{r}_1, \mathbf{r}_2)$ is a function of the positions of a source charge at \mathbf{r}_1 , and a test charge at \mathbf{r}_2 , and represents the amount of work required to bring the test charge from infinity in the bulk solvent to \mathbf{r}_2 . The test charge is a theoretical charge, and creates no reaction field.

We have described $G(\mathbf{r}_1, \mathbf{r}_2)$ alternatively as the interaction energy between two real charges at \mathbf{r}_1 and \mathbf{r}_2 . In terms of work or free energy this second description of G is equivalent to the definition

$$G(\mathbf{r}_1, \mathbf{r}_2) = W(\mathbf{r}_1, \mathbf{r}_2) - W(\mathbf{r}_1) - W(\mathbf{r}_2) \quad (\text{II.12})$$

In this equation $W(\mathbf{r})$ is the work required to bring a single real charge to \mathbf{r} in the presence of the foreign dielectric and therefore includes work done against image charges, and $W(\mathbf{r}_1, \mathbf{r}_2)$ is the work required to bring up two real charges. We note parenthetically that $W(\mathbf{r}_1)$ may be computed from $G(\mathbf{r}_1, \mathbf{r}_2)$, the latter obtained as a solution to Poisson's equation or the Debye-Hückel equation. The physical meaning of $W(\mathbf{r}_1)$ as the increment in self-energy due to the foreign dielectric implies

$$W(\mathbf{r}_1) = \lim_{\mathbf{r}_2 \rightarrow \mathbf{r}_1} [G(\mathbf{r}_1, \mathbf{r}_2) - G_D(r_{12})] \quad (\text{II.13})$$

where $G_D(r_{12})$ is the Green's function for bulk solvent. Our specific G for the cylinder is the work required to bring two charges initially far apart along the cylinder, but at fixed radial distances from the axis, to some arbitrary relative separation. We expect that $W(\mathbf{r})$ will become infinite if \mathbf{r} approaches the surface of a body with $D_0 < D$, but this phenomenon is to be distinguished from the behavior of the interaction G .

Next we give a textbook example of the ratio $R = G(\mathbf{r}_1, \mathbf{r}_2)/G_D(r_{12})$, shown in Figure 1 for the cylinder. For two charges on or very near the surface of a dielectric sphere in a salt-free medium, and separated by polar angle θ , Stratton's solution¹¹ may be used to verify the following properties of $R(\theta)$. $R(0^\circ) = 2D/(D + D_0)$, in agreement with our results for a cylinder, or textbook results for a plane boundary. And $R(180^\circ) = 0.6$, plausibly greater than what Figure 1 gives for the cylinder (0.53), but still less than unity.

III. Helical Array of Charges

In view of the quite large effect of a cylinder on the interaction between point charges on its surface, especially at high concentrations of salt, we have examined the self-energy of helical distributions of charge. Specifically, the question put in this section is whether the calculated effect of varying salt concentration on the self-energy differs between the helical array and a uniform surface distribution of charge. The potential on the surface, that is, the self-energy, does not depend on D_0 for the uniform distribution. Of course there are further approximations to the uniform distribution, such as the continuous line of charge, that also affect the self-energy at high salt concentrations.

The charges in a helical array are located at discrete values of z in the cylindrical polar coordinates (z, a, ϕ) , where $\phi = 2\pi z/p$, and p is the pitch. For DNA p/a is about 3.45, and for an α helix, p/a is about 0.68. As the pitch increases, a helical charge distribution goes over to a line of charges parallel to the cylinder axis, and reaches the maximum degree of nonuniformity with respect to varying pitch.

The interaction G between two charges separated by a distance z along the cylinder axis is given in eq II.5 or II.11, and the potential Ψ is defined as the sum of such pair interactions:

$$\Psi = \sum_j G(\kappa, z_j) \quad (\text{III.1})$$

The sums could be handled straightforwardly with the aid of formulas for G given in the Appendix, but it would be much easier if the sums could be converted to integrals, and appropriate modifications of eq III.1 will be made to

Table I^a

κ	unif	$\theta = 0$	$\theta = \pi$	av
(a)				
0.1	0.387	0.387	0.387	0.387
0.2	0.288	0.288	0.289	0.288
0.4	0.200	0.198	0.202	0.200
0.6	0.156	0.151	0.160	0.155
0.8	0.129	0.119	0.135	0.127
1.0	0.110	0.096	0.120	0.108
1.2	0.096	0.077	0.109	0.093
1.4	0.085	0.060	0.102	0.081
1.6	0.077	0.046	0.097	0.071
1.8	0.070	0.033	0.093	0.063
2.0	0.064	0.021	0.091	0.056
(b)				
0.1	-0.938	-0.943	-0.935	-0.939
0.2	-0.865	-0.873	-0.860	-0.866
0.4	-0.739	-0.771	-0.717	-0.744
0.6	-0.644	-0.710	-0.597	-0.654
0.8	-0.569	-0.680	-0.494	-0.587
1.0	-0.511	-0.669	-0.405	-0.537
1.2	-0.463	-0.671	-0.329	-0.500
1.4	-0.423	-0.679	-0.265	-0.472
1.6	-0.390	-0.691	-0.212	-0.451
1.8	-0.361	-0.704	-0.168	-0.436
2.0	-0.337	-0.717	-0.132	-0.425

^a The self-energy $(2\pi/\beta)\Delta\Psi$ and its derivative $(D/2\beta)\times d\Delta\Psi/d\ln\kappa$ are given in parts (a) and (b), respectively, for a helical stripe of charge in phase ($\theta = 0^\circ$) and out of phase ($\theta = 180^\circ$) with the test charge on a cylindrical surface of radius $a = 1$. The pitch $p = 3.45$ corresponds to DNA, and $D_0 = 2$, $D = 80$. The column labeled "unif" gives the value for a uniformly charged cylinder. The column labeled "av" is the average of values for 0° and 180° , and corresponds to the cylindrical model of double stranded DNA. For a continuous line of charge the normalized derivative would have value $(D/2\beta)d\Delta\Psi/d\ln\kappa = -1$.

permit this simplification. As the equation stands, conversion to an integral would give the potential acting on a charge contained in a continuous helix, and this potential is infinite. We therefore add and subtract a comparison potential evaluated for vanishing salt concentration, and write

$$\Psi = \Delta\Psi + \Psi^0 \quad (\text{III.2})$$

$$\Psi^0 \equiv \sum_j G^0(0, z_j) \quad (\text{III.3})$$

$$\Delta\Psi \equiv \sum_j [G(\kappa, z_j) - G^0(0, z_j)] \quad (\text{III.4})$$

If Ψ^0 were simply the potential Ψ evaluated for $\kappa = 0$, the summand in (III.4) would converge at $z = 0$, but would diverge at large z , and the desired integral over z could not be extended to infinity. We therefore define Ψ^0 to be the potential for $\kappa = 0$, less the potential due to a uniformly charged cylinder at $\kappa = 0$. This subtraction will correspond to the omission of an $m = 0$ term in eq II.5. We now have a definition of $\Delta\Psi$ which allows the sum to be replaced by an infinite integral. The reference potential Ψ^0 is independent of salt concentration, and the effect of varying κ is contained entirely in $\Delta\Psi$. The latter will separate naturally, in the continuous limit, into the potential of a continuous charge distribution, and corrections that depend on the pitch.

Equations II.5 and III.4 in the continuous limit give

$$\Delta\Psi = (\beta/4\pi^2) \sum_{m=-\infty}^{\infty} \int_{-\infty}^{\infty} dk \int_{-\infty}^{\infty} dz (g_m - g_m^0) \exp(ikz + im\phi) \quad (\text{III.5})$$

where β is the charge density per unit length of axis, and

$$\phi = \theta + 2\pi z/p \quad (\text{III.6})$$

A phase shift θ has been included in order to accommodate the effect of a double strand of charges on DNA. (Either $\theta = 0^\circ$, in which case the term $z = 0$ should be omitted from (III.3), or $\theta = 180^\circ$, in which case all charges are to be included in the sum.) In the continuous limit for $\Delta\Psi$, eq III.5 applies for all θ .

A delta function may be recognized to give

$$\Delta\Psi = (\beta/2\pi)[g_0(0) + 2 \sum_{m=1}^{\infty} \Delta g_m \cos m\theta] \quad (\text{III.7})$$

where

$$\Delta g_m \equiv g_m(2\pi m/p) - g_m^0(2\pi m/p) \\ g_0(0) = 4\pi K_0(\kappa a)/aD\kappa K_1(\kappa a) \quad (\text{III.8})$$

Here the displayed argument of g_m is the value of k . A superscript zero indicates that $\kappa = 0$, its absence indicates that the actual value of κ should be used. The required values of g_m are easily computed from eq II.8 and II.9. The corrections are extremely small, as a brief consultation of Table I will verify.

Similar support for the uniformly charged cylinder model has been presented by Bailey.¹²

Acknowledgment. This work was supported in part by NIH Grant GM13556.

IV. Appendix

The practical calculation of the potential from eq II.8-II.11 will be surveyed here.

The first problem is to determine the coefficients H_m for large m . Values for large m are required only for small z , and may be obtained from the uniform asymptotic expansions listed in Abramowitz and Stegun.¹⁰ These are expansions in inverse powers of m . Their substitution into the expression for H , eq II.11, gives

$$H_m = \frac{2|z|}{\pi(D_0 + D)} \left[K_0(m|z|) - \frac{(D - D_0)}{(D + D_0)} \left(\frac{\pi}{8m} \right) \times \right. \\ \left. (1 - m|z|) \exp(-m|z|) + \dots \right] \quad (\text{A1}) \\ a \equiv 1$$

The details of the derivation of this formula from the original integral over k in eq II.11 show that the leading terms in the expansion originate from large values of k and that consequently they are independent of κ . For $\phi = 0$, this formula may be used to derive the limiting result for zG as $z \rightarrow 0$, as quoted in the main text. In this limit the sum over m can be replaced by an integral.

For small z and m not too large, direct numerical integration of the integral expression for H_m in eq II.11 is practical. For large z a contour deformation of the path of integration is desirable. The path originally runs along the real axis, and deformation of it to run along the two sides of the positive imaginary axis gives exponential convergence of the integrand for large z . In justification of this deformation, we note first that the Bessel functions themselves are analytic throughout the k plane. The square root functions that define l and l_0 in terms of k have branch cuts along the imaginary axis, but the real parts of l and l_0 are never negative. Asymptotic forms for the Bessel functions in the right half of the l or l_0 planes indicate adequate convergence at infinity for the H_m integrand, and the only uncertainty remaining is whether the latter has any poles off the coordinate axes. A formal proof of their absence is sketched at the end of the Appendix. A numerical proof of their absence lies in the

agreement between the two expressions for H_m in the region of intermediate z (ca. $z = 0.5$), where both are practical.

The result of the contour deformation, appropriate transformation of the Bessel functions from real to imaginary arguments, and considerable rearrangement, is

$$H_m = \frac{2|z|}{\pi} \int_{\kappa}^{\infty} \frac{(BC - AE)}{C_2 + E^2} \exp(-R|z|) dR \quad (\text{A2})$$

where

$$A = J_m(R)J_m(S\rho); \quad S \equiv (R^2 - \kappa^2)^{1/2}; \quad a = 1$$

$$B = -J_m(R)Y_m(S\rho)$$

$$C = DJ_m(R)SJ_m'(S) - D_0J_m(S)RJ_m'(R)$$

$$E = -DJ_m(R)SY_m'(S) + D_0Y_m(S)RJ_m'(R)$$

$$BC - AE \rightarrow (2D/\pi)[J_m(R)]^2 \text{ as } \rho \rightarrow a = 1$$

Equation A2 also requires certain precautions in the numerical integration, because of the rapid variation of the integrand in the vicinity of the zeros of $J_m(R)$. For small z the integrand converges slowly, the integral must be extended to large z , and a great many zeros require special treatment.

Our procedure was to use eq A2 for m up to 10, and to supplement these values with the asymptotic form, eq A1, when necessary for the smaller values of z .

We now return to the possible poles of g_m in the k plane. We are indebted to Professor Ira Bernstein for suggesting the lines of our argument. In eq II.6, let $D(\rho)$ be replaced by a continuous function of arbitrary steepness, and the interval $(0, \infty)$ by a finite interval. At the right boundary g_m vanished, and at the left $dg_m/d\rho$ vanishes. Then

$$(\mathcal{L} + k^2)g_m = 4\pi\delta(\rho - a)/aD(\rho) = s(\rho) \quad (\text{A3})$$

where

$$\mathcal{L}g_m \equiv -\frac{1}{\rho D(\rho)} \frac{\partial}{\partial \rho} \left(\rho D(\rho) \frac{\partial g_m}{\partial \rho} \right) + \left(\kappa^2(\rho) + \frac{m^2}{\rho^2} \right) g_m \quad (\text{A4})$$

The operator \mathcal{L} is self-adjoint and positive definite for a scalar product defined with weight function $\rho D(\rho)$. Consequently \mathcal{L} has a complete set of eigenfunctions f_i and positive eigenvalues λ_i , and the source and Green's function may be expanded as follows:

$$s(\rho) = \sum s_i f_i; \quad g_m = \sum s_i f_i / (k^2 + \lambda_i) \quad (\text{A5})$$

it follows that g_m can have only imaginary poles. These generate a branch cut as the limits on ρ are extended to zero and infinity.

References and Notes

- (1) J. G. Kirkwood and F. H. Westheimer, *J. Chem. Phys.*, **6**, 506 (1938).
- (2) F. H. Westheimer and J. G. Kirkwood, *J. Chem. Phys.*, **6**, 513 (1938).
- (3) F. P. Buff, N. S. Goel, and J. R. Clay, *J. Chem. Phys.*, **63**, 1367 (1975).
- (4) D. L. Beveridge and G. W. Schnuelle, *J. Phys. Chem.*, **79**, 2562 (1975).
- (5) F. R. Harris and S. A. Rice, *J. Chem. Phys.*, **25**, 955 (1956).
- (6) T. L. Hill, *Arch. Biochem. Biophys.*, **57**, 229 (1955).
- (7) G. Manning, *Biophys. Chem.*, **7**, 95 (1977), and earlier work cited there.
- (8) A. D. MacGillivray, *J. Chem. Phys.*, **57**, 4071, 4075 (1972), and earlier work cited there.
- (9) J. Skolnick, Ph.D. Thesis, Yale University, 1978.
- (10) M. Abramowitz and I. A. Stegun, "Handbook of Mathematical Functions", Dover Publications, New York, N.Y., 1972. We use their notation for all Bessel functions, J, Y, I, K .
- (11) J. A. Stratton, "Electromagnetic Theory", McGraw-Hill, New York, N.Y., 1941, p 204, eq 20.
- (12) J. M. Bailey, *Biopolymers*, **12**, 559 (1973).

Pressure Dependence of Upper Critical Solution Temperatures in the System Polystyrene–Cyclopentane

Maki Ishizawa,^{1a} Nobuhiro Kuwahara,^{*1b} Mitsuo Nakata,^{1a} Wataru Nagayama,^{1a} and Motozo Kaneko^{1a}

Department of Polymer Science, Faculty of Science, Hokkaido University, Sapporo, Japan, and Department of Polymer Science, Faculty of Technology, Gunma University, Kiryu, Japan. Received April 26, 1978

ABSTRACT: The pressure dependence of the upper critical solution temperature (ucst) in solutions of polystyrene in cyclopentane has been measured over the pressure range of 0.1 to ~70 MPa. The values of $(dT/dP)_{c,P=0}$ for the ucst of polystyrene ($M_w \times 10^{-4} = 67$ and 200) in cyclopentane are negative (-0.398 and -0.480 deg MPa⁻¹). The magnitude of $(dT/dP)_c$ at constant composition gradually decreases with increasing pressure over 0.1 to ~70 MPa. The pressure dependence of the ucst in the polystyrene–cyclopentane is examined through the χ_1 parameter derived by Patterson and Delmas in conjunction with the equations of state by Flory.

The recent theories of polymer solution thermodynamics by Patterson²⁻⁶ and Flory⁷⁻¹⁰ qualitatively predict both the upper critical solution temperature (ucst) and the lower critical solution temperature (lcst). The importance of the free volume effect or "equation of state" contribution in the polymer solution has been recognized because of the general appearance of the lcst in nonpolar polymer solutions,¹¹⁻¹⁸ the pressure dependence of the ucst and lcst,¹⁹⁻²⁵ the negative excess volume of mixing,²⁶⁻³² and the composition dependence of χ .^{27-31,33-36}

Saeki et al.¹⁵ found a pair of the θ_u and θ_l in a convenient temperature range in the system polystyrene–cyclopentane. Since contribution of the free volume term to χ_1 is beyond 40% at the θ_u ,¹⁵ a considerable lowering of the ucst with increase of pressure is expected even in the temperature region of the ucst. Examinations of the pressure dependence of the ucst and lcst under high pressure are of great importance in understanding thermodynamic properties of polymer solutions. The present work was done to supply the $(P, T, \text{composition})$ phase diagram for